Inosine can increase DNA's susceptibility to photo-oxidation by a Ru(II) complex due to structural change in the minor groove

Article

Accepted Version

CHEMISTRY
A European Journal

A Journal of
ChemPubSoc Europe

Accepted Article

Title: Inosine can increase DNA's susceptibility to photo-oxidation by a Ru(II) complex due to structural change in the minor groove

Authors: John M. Kelly, Paraic Keane, James Hall, Fergus Poynton, Bjorn Poulsen, Sarah Gurung, Ian Clark, Igor Sazanovich, Michael Towrie, Thorfinnur Gunnlaugsson, Susan Quinn, and Christine Cardin

To be cited as: *Chem. Eur. J.* 10.1002/chem.201701447

Link to VoR: http://dx.doi.org/10.1002/chem.201701447

Supported by ACES

WILEY-VCH

WILEY-VCH

FULL PAPER

Inosine can increase DNA's susceptibility to photo-oxidation by a Ru(II) complex due to structural change in the minor groove

Páraic M. Keane,*[ab] James P. Hall,[ac] Fergus E. Poynton,[bd] Bjørn C. Poulsen,[bd] Sarah P. Gurung,[ac] Ian P. Clark,[e] Igor V. Sazanovich,[e] Michael Towrie,[e] Thorfinnur Gunnlaugsson,[bd] Susan J. Quinn,*[f] Christine J. Cardin,*[a] and John M. Kelly*[b]

Abstract: Key to the development of DNA-targeting phototherapeutic drugs is determining the interplay between the photoactivity of the drug and its binding preference for a target sequence. For the photo-oxidising lambda-[Ru(TAP)$_2$(dppz)]$^{2+}$ (Λ-**1**) complex bound to either d{$T_1C_2G_3G_4C_5G_6C_7C_8G_9A_{10}$}$_2$ (**G9**) or d{TCGGCGCCIA}$_2$ (**I9**), the X-ray crystal structures shows the dppz intercalated at the terminal T_1C_2;G_9A_{10} step or T_1C_2;I_9A_{10} step. Thus substitution of the G_9 nucleobase by inosine does not affect intercalation in the solid state although with **I9** the dppz is more deeply inserted. In solution it is found that the extent of guanine photo-oxidation, and the rate of back electron transfer, as determined by ps and ns time-resolved infrared and transient visible absorption spectroscopy, is enhanced in **I9**, despite it containing the less oxidisable inosine. This is attributed to the nature of the binding in the minor groove due to the absence of an NH_2 group. Similar behaviour and the same binding site in the crystal.are found for d{TTGGCGCCAA}$_2$ (**A9**), In solution we propose that intercalation occurs at the C_2G_3;C_8I_9 or T_2G_3;C_8A_9 steps, respectively, with G_3 the likely target for photo-oxidation. This demonstrates how changes in the minor groove (in this case removal of an NH_2 group) can facilitate binding of Ru(II)dppz complexes and hence influence any sensitised reactions occurring at these sites. No similar enhancement of photooxidation on binding to **I9** is found for the delta enantiomer.

[a] P. M. Keane, J. P. Hall, S. P. Gurung, C. J. Cardin
Department of Chemistry, University of Reading, Whiteknights, Reading, RG66AD, UK
E-mail: c.j.cardin@reading.ac.uk
[b] P. M. Keane, F. E. Poynton, B. C. Poulsen, T. Gunnlaugsson, J. M. Kelly
School of Chemistry, Trinity College Dublin, Dublin 2, Ireland
E-mail: keanepa@tcd.ie, jmkelly@tcd.ie
[c] J. P. Hall, S. P. Gurung
Diamond Light Source, Harwell Science and Innovation Campus, Didcot, Oxfordshire, OX11 0DE, UK
[d] F. E. Poynton, B. C. Poulsen, T. Gunnlaugsson
Trinity Biomedical Sciences Institute, Pearse St., Dublin 2, Ireland
[e] I. P. Clark, I. V. Sazanovich, M. Towrie
Central Laser Facility, Research Complex at Harwell, STFC Rutherford Appleton Laboratories, Didcot, Oxfordshire, OX11 0QX, UK
[f] S. J. Quinn
School of Chemistry, University College Dublin, Belfield, Dublin 4, Ireland
Email: susan.quinn@ucd.ie

Supporting information for this article is given via a link at the end of the document.

Introduction

Recent studies have shown that inosine[1] is responsible for several important effects in nucleic acid chemistry. For example biological diversity has been linked to posttranscriptional RNA editing which involves the deamination of adenosine to inosine.[2] In double-stranded nucleic acids inosine forms Watson Crick base-pairs with cytosine and can therefore replace guanine. However substitution of a GC base-pair with an IC has been found to influence the thermal stability of DNA in a highly sequence dependent manner[3,4] and replacing guanosine with inosine is also reported to influence the structural conformation of DNA beyond the local site of substitution.[4] Another conspicuous feature of this process is that, while the groups in the major groove of B-DNA are similar for GC and IC they are quite different in the minor groove. In fact, the minor groove surfaces of I-C and A-T are closely similar (Figure 1). This may have important consequences for the non-covalent binding of drugs and other small molecules and this has been demonstrated for compounds such as the pluramycin family of alkylating compounds,[5a-b] daunomycin,[5c] quinoxaline antibiotics[5d-e] and echinomycin.[5d]

Ruthenium polypyridyl complexes have been shown to be avid binders to DNA with potential applications for imaging and for phototherapeutics.[6] Particularly important amongst these are complexes containing the dipyridophenazine (dppz) ligand, which can intercalate between the base pairs of DNA. Some of these act as DNA 'light switches'.[7] Others, such as [Ru(TAP)$_2$(dppz)]$^{2+}$ (**1**, Figure 1) (TAP = 1,4,5,8-tetraaza-phenanthrene), may photo-oxidise guanine by one-electron transfer to the photoexcited complex.[8] The TAP ligand can also form covalent adducts with guanine under certain conditions,[9] while **1** and its modified analogues have recently been shown to cause light-induced cytotoxicity against HeLa cancer cells.[10]

Understanding the mechanism of photosensitised DNA damage, and therefore developing targeted drug therapies, requires accurate knowledge of where and how the sensitiser is bound in the DNA. In this regard X-ray crystallography can provide critical information about the interactions in the binding site and is increasingly proving very informative in defining the mode and geometry of binding of polypyridyl Ru(II)dppz complexes.[11] This was recently demonstrated for Λ-[Ru(TAP)$_2$(dppz)]$^{2+}$ (Λ-**1)** where X-ray crystallography of the isosteric Λ-[Ru(phen)$_2$(dppz)]$^{2+}$ bound to the oligodeoxynucleotides (ODNs) d{CCGGTACCGG}$_2$ or d{CCGGATCCGG}$_2$[11b] proved to be an excellent guide to the preferred binding site and hence the electron transfer properties monitored by transient spectroscopy in solution.[8f] In a further important development, we reported the first time-resolved infrared (TRIR) study performed directly in the crystal,[12] where

10.1002/chem.201701447
WILEY-VCH

we were able to use precise knowledge of the binding geometry to assign G_9 as the oxidation site for Λ-**1** intercalated at the terminal T_1C_2;G_9A_{10} step of d{TCGGCGCCGA}$_2$ (**G9**) in the crystal.

Inosine is reported to have an oxidation potential *ca.* 200 mV higher than G.[13a] Hence G/I replacement has been used as a control experiment to study the dynamics of ET in DNA.[13] In the event of the G_9 site in **G9** being the target in solution a reduced yield (and/or rate) of photoinduced electron transfer (PET) for **I9** in solution would be anticipated. To the best of our knowledge, there is no structural data available, which allows a comparison of the intercalation geometry at the base-pairs GC, IC and AT for any DNA-binder. For the lambda enantiomers of $[Ru(TAP)_2(dppz)]^{2+}$ or $[Ru(phen)_2(dppz)]^{2+}$ it has been established that angled intercalation from the minor groove is the preferred binding mode at any of the ten DNA steps with the exception of the TA/TA step.[11]

As noted above, an IC and GC basepair present the same functional groups in the major groove, while from the minor groove it is the IC and AT basepairs which are the same (Figure 1). In this paper, we consider the effect of replacement of guanine by inosine on the binding of Λ-$[Ru(TAP)_2(dppz)]^{2+}$ both in the crystal and in solution and the consequences of this substitution on the primary photooxidation properties as monitored by nanosecond and picosecond transient absorption (TrA) and time-resolved infra-red (TRIR) methods.

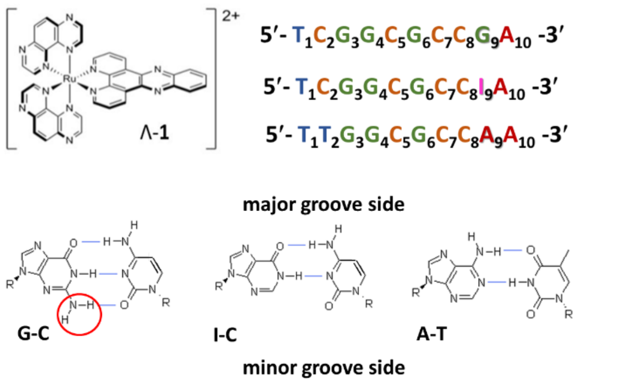

Figure 1. Λ-$[Ru(TAP)_2(dppz)]^{2+}$ (Λ-**1**) and oligonucleotides used in this study. Colour code for structural figures throughout I – pink, G – green, C -yellow, A - red, T – blue. The GC, IC and AT base pairs are shown with respect to the major and minor grooves of DNA.

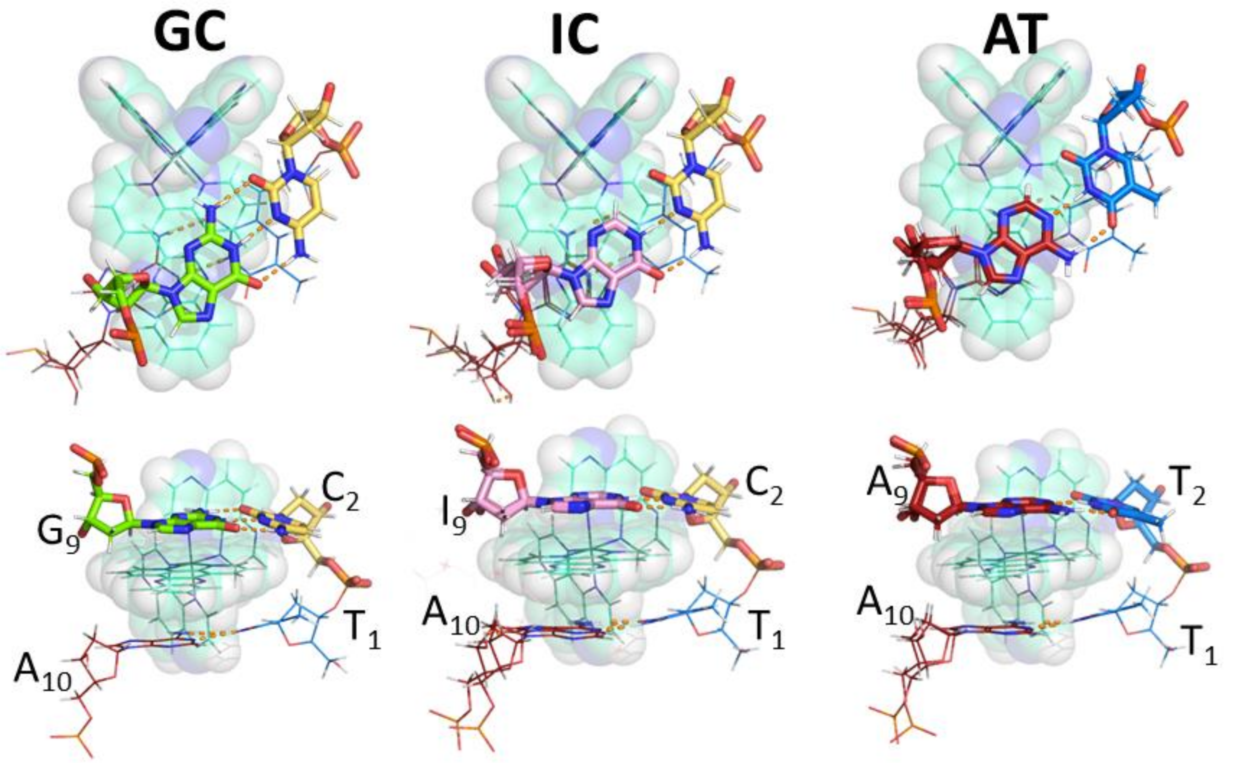

Figure 2. A comparison of the intercalative binding sites for the three sequences compared in this study. The upper panels show the projection on to the dppz plane on the G_9C_2/I_9C_2/A_9T_2 side of the cavity. The lower panels show the view from the major groove along the long axis of the dppz ligand and with the residues labelled. The terminal base-pair is shown as thin lines in each case, and with the disorder present at the A_{10} residue also shown. The lambda enantiomer (Λ-**1**) is shown in green, as lines with a partially transparent space-filling model superimposed. All hydrogen atoms are included in calculated positions.

10.1002/chem.201701447

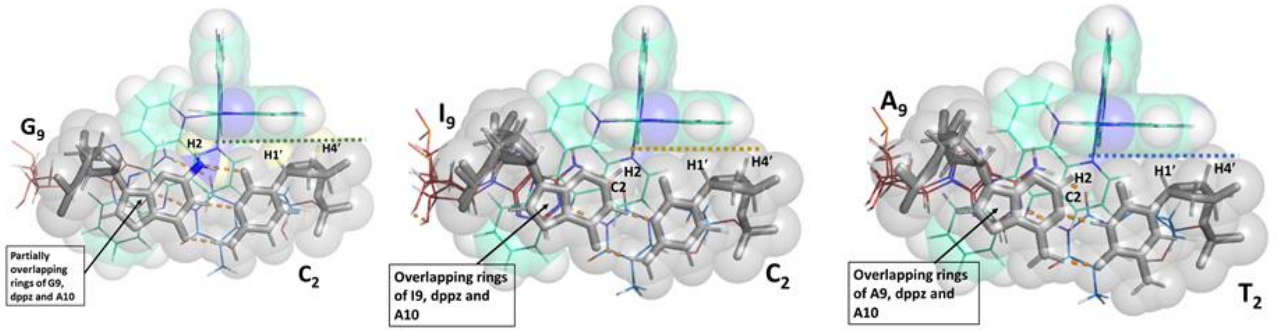

Figure 3. Structural features determining the orientation of the metal complex in the DNA cavity for the three structures compared. The contact surface between the TAP ancillary ligand and the pyrimidine sugar at position 2 of the sequence is shown as a dashed line. The nucleic acid component is shown as grey sticks with partially transparent space-filling model superimposed. The metal complex is rendered as in Figure 2. The projection is a rotation of that in Figure 2 to make the TAP ligand horizontal.

Results

X-ray crystal structures of (Λ-1) with d{TCGGCGCCIA}$_2$ (I9) and d{TTGGCGCCAA}$_2$ (A9)

Crystals of Λ-**1** with **I9** and **A9** could be best obtained by starting with the pure enantiomer, in contrast to the **G9** analogue, which is sufficiently selective to efficiently crystallise from *rac*-**1**. The data from the Λ-**1**- **I9** crystal was of particularly high quality with a resolution of 0.96 Å, close to small molecule precision. Each of the structures show intercalation of the metal complex from the minor groove at the terminal site (*i.e.* $T_1C_2;G_9A_{10}$ for **G9,** $T_1C_2;I_9A_{10}$ for **I9** and $T_1T_2;A_9A_{10}$ for **A9**), as well as semi-intercalation of a TAP between G_3 and G_4 (Figure S1 & S2).

The high quality of the data (in the top 1% of structures in the PDB) allows detailed structural comparisons of the intercalation site in the three systems. A key factor determining the precise orientation of each of the metal complexes is contacts between the pyrimidine deoxyribose ring and the TAP ancillary ligand (Figure 3), for example H1′ touches the C10 of the TAP ring, as measured by the C1′-C10 contact distance (SI Figures S3-S5). In the case of **G9**, the projecting 2-NH_2-group of the purine reduces the area of the contact surface, with one H atom (labelled H2 in Figure 3) becoming the second important contact. A consequence of this is that the overlap between the pyrazine ring of the dppz ligand and the purine rings on either side is only partial when the purine is guanine, giving a weaker hydrophobic interaction.

Inosine presents a smoother contour in the minor groove, increasing the contact surface although the cytosine C1′-TAP(C10) distance is only 0.07Å less than in **G9**. As shown in Figure 3, there is much better overlap between the purine and the pyrazine rings. Another feature is a decrease of 0.45 Å in the Ru-centroid distance for the purine six-membered rings for **I9** compared to **G9**. For the Ru-cytosine centroid this is only 0.09 Å, so that the difference is mainly in the purine location. By contrast the cytosine ring position, as well as the sugar-TAP contact surface, change very little. All these comparisons point to the tighter interaction at an IC step compared to a GC step. The comparison of the IC with an AT base-pair shows a much higher degree of similarity, with a slight lengthening of the thymine C1′-TAP(C10) distance (but only by 0.04 Å), and an increase of 0.1 Å in the Ru-purine centroid distance compared to **I9**. In the **A9** case the purine-pyrazine ring stacking is greatest of all the three pairs studied.

Binding studies of Λ-[Ru(TAP)$_2$(dppz)]$^{2+}$ in the presence of G9 I9 and A9 in solution

Comparative UV/vis and emission binding titrations were performed for Λ-**1** in the presence of **G9**, **I9** and **A9** in 50 mM phosphate buffer. In a similar fashion to what was found for other oligonucleotides,[8f] upon addition of the ODN the absorption spectra show a characteristic reduction in absorbance at 412 nm and a slight shift in the band maximum to 420 nm. Simultaneously the emission band at 635 nm is strongly reduced due to quenching of the excited state upon binding to the ODN (ESI Figure S6). Figure 4a shows the diminution of the emission intensity in each of these solutions. Binding constants were determined from these luminescence data (ESI Section S3 & Table S2) using a modified method of that reported by Carter *et al*.[14] It may be noted that binding is much stronger for **I9** (13 x 10^5 M^{-1}) and **A9** (11 x 10^5 M^{-1}) than it is for **G9** (5.3 x 10^5 M^{-1}).

10.1002/chem.201701447

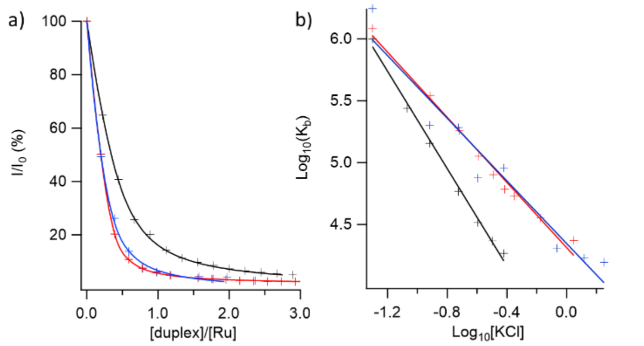

Figure 4. (a) Change in emission intensity, and corresponding binding fits, for Λ-**1** in the presence of **G9** (black) **I9** (red) and **A9** (blue) (b) Linear fits to determine ΔG (non-electrostatic) for Λ-**1** in the presence of **G9** (slope = 1.97), **I9** (slope = 1.30) and **A9** (slope = 1.27). In H_2O in 50 mM phosphate buffer pH S9

Titrations were also carried out in solutions containing additional KCl (100 mM and 500 mM), and these revealed significant decreases in binding affinity at higher ionic strength (ESI Figure S7). To further investigate the effect of ionic strength on binding, the recovery of the emission was monitored when KCl was added gradually to a solution containing Λ-**1** fully bound to the relevant ODN. The resulting plots (Figure 4b) may be used to determine the dependence of the binding on electrostatic and non-electrostatic components.[15] The derived values for ΔG(non-electrostatic) are -19.3 kJ mol^{-1}, -24.7 kJ mol^{-1} and -24.8 kJ mol^{-1} for binding to **G9**, **I9** and **A9**, respectively. This is consistent with a larger hydrophobic interaction with **I9** and **A9**, which, in light of the structural data, could be due to a greater degree of overlap between the dppz and the base-pairs of the intercalation pocket.

Circular dichroism (CD) has been widely used to study the interaction of small molecules, including ruthenium polypyridyls, with DNA.[16] Figures S8 (a) and (c) show that the binding of Λ-**1** causes very similar changes for **I9** and **G9** consistent with the binding modes being similar.

Comparison of photo-oxidation by Λ-[Ru(TAP)$_2$(dppz)]$^{2+}$ bound to G9, I9 and A9 ODNs using transient spectroscopic methods

To study the reversible photo-oxidation of guanine and the accompanying reduction of the metal complex we have used ultrafast time-resolved spectroscopy, following the approach already reported for Λ-**1** bound to **G9**.[8e] Experiments were performed in D_2O at a [Ru]/[duplex] ratio of 0.8:1, where all complexes are expected to be bound.[17] The results of both the TrA and TRIR measurements allow us to determine the relative yield and rates of both the forward (ET) and reverse electron transfer (bET) (Scheme 1). It should be noted that no PET is observed with inosine or adenine polynucleotides.[18]

$$[Ru^{II}(TAP)_2(dppz)]^{2+} \xrightarrow{MLCT} [Ru^{III}(TAP)(TAP^{\bullet-})(dppz)]^{2+*}$$
$$[Ru^{III}(TAP)(TAP^{\bullet-})(dppz)]^{2+*} + G \xrightarrow{ET} [Ru^{II}(TAP)(TAP^{\bullet-})(dppz)]^{+} + G^{\bullet+}$$
$$[Ru^{II}(TAP)(TAP^{\bullet-})(dppz)]^{+} + G^{\bullet+} \xrightarrow{bET} [Ru^{II}(TAP)_2(dppz)]^{2+} + G$$

Scheme 1. A mechanism for the photo-oxidation of G by [Ru(TAP)$_2$(dppz)]$^{2+}$

Picosecond TrA measurements show that 400 nm laser excitation initially generates the MLCT state of the complex, which can be observed as a broad absorption at 600 nm (Figure 5a and Figure S11). The forward ET can then be monitored by the formation of the reduced [Ru(II)(TAP)(TAP$^{\bullet-}$)(dppz)]$^{+}$ complex at 515 nm (Figure 5a,b and ESI Figure S11a-c). It can be seen that there is a markedly higher yield of the reduced complex in the presence of **I9** or **A9**. A relative yield enhancement of *ca.* 70% was calculated using the signal at 460 nm (*i.e.* in the negative signal 'bleach' region) (see ESI section S5).

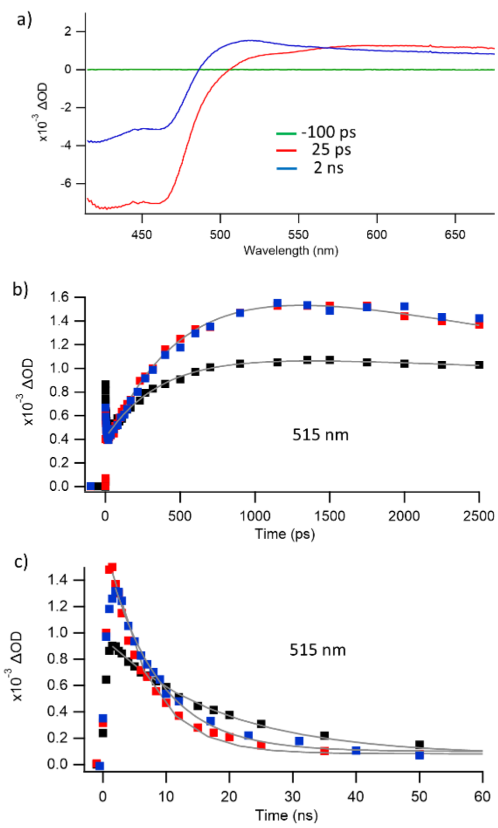

Figure 5. (a) Ps-TrA spectra of 400 µM Λ-**1** bound to **I9** (500 µM duplex) at selected delays after excitation (λ_{exc} = 400 nm, 50 fs, 1 µJ) (b) Comparison of fitted kinetic traces at 515 nm for forward ET on ps timescale for Λ-**1** bound to **G9** (black), **I9** (red) and **A9** (blue) (c) Comparison of fitted monoexponential traces at 515 nm for reverse ET on ns timescale (λ_{exc} = 355 nm, < 1 ns, 1 µJ). In 50 mM phosphate buffered D_2O (pH 7).

The rate of the forward ET was obtained by fitting the grow-in of the reduced metal complex to an exponential function (taking account of the subsequent decay process). This gives rate constants of k = 1/490 ps^{-1} for **I9** and 1/510 ps^{-1} for **A9**, which are close to that previously reported for **G9** (1/410 ps, see Table 2).[8e] TrA experiments were also carried out on the nanosecond timescale (355 nm excitation) in order to monitor the subsequent back ET (bET). For Λ-**1** bound to **I9** and **A9**, the signal of the reduced species decays significantly faster (7 ns and 8 ns, respectively) than it does for **G9** (τ = 17 ns; see Figure 5c and SI Figure S11d-f).

10.1002/chem.201701447

WILEY-VCH

The TRIR technique allows one to probe directly changes in the nucleobases and hence provides an excellent method for monitoring the oxidation of guanine.[19] In the ps-TRIR spectra of Λ-**1** bound to **G9**, **I9** or **A9**, strong bleaching is observed at 1650 cm^{-1} and 1680 cm^{-1}, where the C=O absorptions of C and G occur, respectively. In the presence of **I9** or **A9**, the relative bleach intensity is greater than in **G9** (see Figure 6 and ESI Figure S12a,b). There is also more prominent absorption at *ca.* 1700 cm^{-1} for **I9** and **A9**, which may be assigned to the guanine radical cation.[19] The more defined signal for **I9** and **A9** compared to **G9** is due to the higher yield in the former cases but may also reflect oxidation at a different site (see later). The G bleach band grows in at a rate of 1/605 ps^{-1} for **I9** and 1/510 ps^{-1} for **A9**, similar to that with **G9** (1/460 ps, taking account of the slow recovery noted at longer times; see also ESI Figure S13). These rates are similar to those recorded by ps-TrA for reduction of Λ-**1**, implying that the process observed by TRIR corresponds to oxidation of guanine by the photoexcited Ru complex.

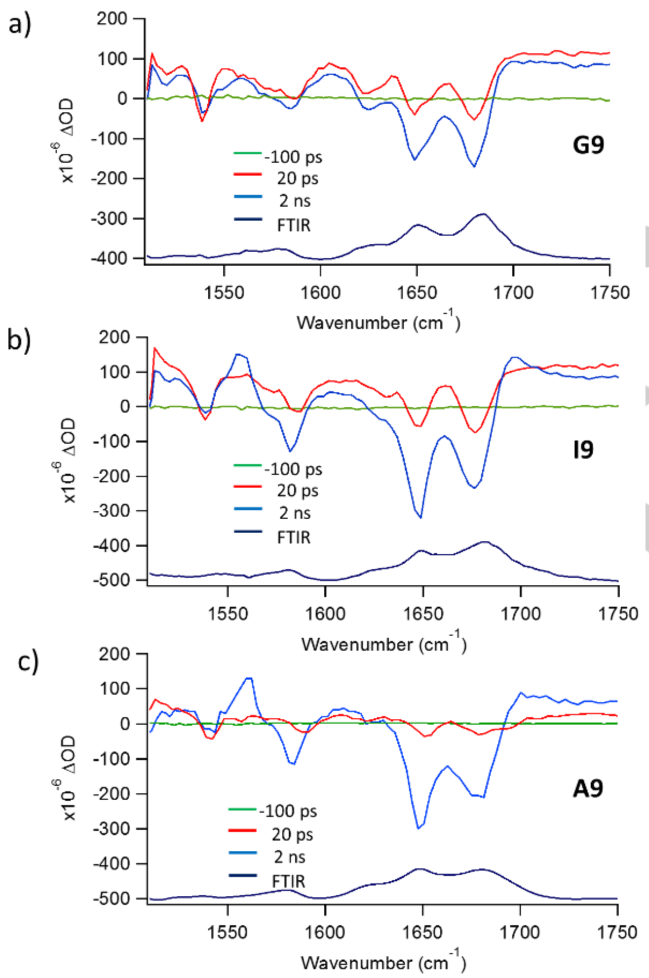

Figure 6. Comparison of ps-TRIR spectra (region of DNA absorption) recorded 20 ps and 2000 ps after laser excitation of 400 μM Λ-**1** in the presence of (a) **G9** (see ref. 8e) (b) **I9** (c) **A9** ([ODN] = 500 μM duplex, λ_{exc} = 400 nm, 50 fs, 1 μJ). Corresponding ground state FTIRs are shown below the spectra. In 50 mM phosphate-buffered D_2O (pH 7)

TRIR spectra in the nanosecond region show the recovery of the C and G carbonyl bleaches, and, most clearly in the case of Λ-**1** with **I9**, the recovery of the transient at 1700 cm^{-1} (see ESI Figure S12c,d). Monoexponential fitting of the bleach recoveries gave lifetimes similar to those recorded by ns-TrA (Table 1 & ESI Figures S14 & S15).

TRIR can also report on the binding site of the complex through interactions of the excited complex with its environment, which results in IR signals from the neighbouring nucleobases.[7,8f,20] At early times (*e.g.* 20 ps) before the oxidation occurs, there is a shoulder at 1695 cm^{-1} in the bleach section of the TRIR spectra of Λ-**1** bound to **A9** that is absent with **G9** or **I9**. This occurs in the region where the thymine C=O ($\nu_{C2=O2}$) is known to absorb (ESI Figure S16),[21] suggesting that the complex could be interacting with a thymine nucleobase in **A9**, which we can assign to the T_2A_9 base pair.

Photo-oxidation by Δ-[Ru(TAP)$_2$(dppz)]$^{2+}$ bound to G9 or I9

UV/Visible and luminescence titrations (Figure S17) show that delta-enantiomer also binds strongly to both **I9** and **G9** but unlike the lambda- enantiomer the binding constants are rather similar (1.3 x 10^5 for **I9** and 1.1 x 10^5 for **G9**.) It may also be noted that the constants for binding to **I9** reveal that there is a much greater affinity for the lambda-enantiomer ((13 x 10^5) than for the delta. Luminescence titrations also demonstrate that the extent of quenching is similar (93%) for this enantiomer when bound to **I9** or **G9** - significantly lower than that found with the lambda-species (98% and 96% respectively)**.**

For the delta-enantiomer transient spectroscopy measurements reveal that the yield of the PET is somewhat lower for **I9** than for **G9,** while the kinetics of both the forward and back reactions are comparable for **G9** and **I9**. (Figures S18 &S19 and Table S4), in contrast to what is found for the lambda-species.

Table 1. Fitted lifetimes and relative ET yields for 400 μM Λ-**1** bound to ODNs **G9**, **I9** and **A9** (500 μM duplex) in 50 mM phosphate buffer in D_2O. Kinetics fitted at single wavelength/wavenumber.

parameter	G9[a]	I9	A9
ps-TrA (515 nm)	410 ± 40 ps	490 ± 50 ps	510 ± 50 ps
ns-TrA (515 nm)	17 ± 3 ns	7 ±1 ns	8 ± 1 ns
ps-TRIR (1650 cm^{-1})	410 ± 60 ps	580 ± 90 ps	500 ± 75 ps
ps-TRIR (1680 cm^{-1})	460 ± 70 ps	605 ± 90 ps	510 ±100 ps
ps-TRIR (1700 cm^{-1})	nd[b]	450 ± 70 ps	390 ± 80 ps
ns-TRIR (1650 cm^{-1})	21 ± 5 ns	9 ± 2 ns	7 ± 2 ns
ns-TRIR (1680 cm^{-1})	15 ± 3 ns	6 ± 1 ns	8 ± 2 ns
Relative ET yield[c]	1	1.7 ± 0.2	1.7 ± 0.2

[a] from ref. 8e [b] nd=not determined due to weak signal [c] determined from bleach at 460 nm, see ESI section S5 for details

Discussion

 10.1002/chem.201701447

WILEY-VCH

The results reported above show that markedly different behaviour is observed in solution for Λ-**1** between **G9** and **I9/A9.** This is especially apparent in the transient measurements and reinforced by the binding studies. By contrast the crystal structures are very similar, all intercalating at site **a**, Figure 7. We have previously shown that the PET with Λ-**1** requires that the dppz be intercalated adjacent to a guanine.[8f] Therefore if the intercalation site is the same in the solution as in the crystal, one might reasonably expect that the yield of ET would be much lower for **I9** or **A9**, as the modified site $T_1C_2;I_9A_{10}$ or $T_1T_2;A_9A_{10}$ in **I9** and **A9** does not contain a guanine. Intriguingly, a strong enhancement of the ET yield was found in solution, as well as a significant increase in the rate of the subsequent back ET. This supports the hypothesis that binding in solution involves a site other than the terminal base-pair step **a**.

Figure 7 shows the five unique steps generated by the self-complementary duplexes. The combination of the photophysical results, together with insights from previous crystallographic measurements, lead us to propose that the predominant binding site for **I9** or **A9** is site **b** in Figure 7.[11] It should be noted that the lambda enantiomer used in this work, and in contrast to the delta enantiomer, will contact the minor groove on the 3′ side of the binding step, and therefore be sensitive to the effect of variation at position 9 of the sequence. By contrast, the other steps will be little affected. Intercalation at a CA/TG site (ie the **b** site of **A9**) may also be favoured by the fact that the stacking interaction of CA/TG is particularly weak (only TA/TA is weaker) and much less than that for CG/CG.[22] This would also be expected to be the case for CI/CG (**b** site of **I9**).

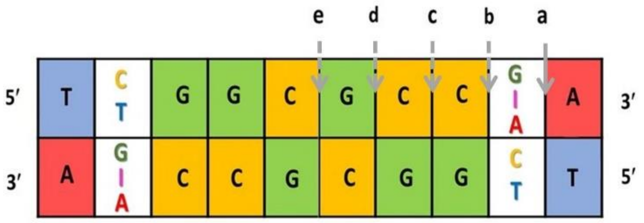

Figure 7. Schematic of the five possible intercalation sites in **G9**, **I9** and **A9**. Sites **a** and **b** are those altered by base substitution. Sites **b** and **e** are equivalent in **G9**

The assignment of site **b** as the preferred binding location is supported by our previously reported finding of a relatively low yield of ET for Λ-**1** bound to the alternating GC duplex $d\{(GC)_5\}_2$.[8e] This suggests that the 5′-GC (site **d**) and 5′-CG (site **e**) steps are not good candidates for strong ET. By contrast, high yields have been recorded where runs of G are present (e.g. in $d\{G_5C_5\}_2$). Sites **b** and **c** both place the complex close to the 5′-G of the GG doublet, which is known to be a ‘hot-spot’ for oxidative damage.[23] An angled intercalation from the minor groove, between G_3 and G_4 (site **c**) would disrupt the GG stacking that is required to lower the oxidation potential of the 5′-guanine, so that we expect that the most efficient ET will occur at site **b**, with the G_3 base being the site of photo-oxidation.

Further evidence that the binding site in solution is different from that in the crystal may be deduced from the TRIR studies (Figure 6). For the **A9** system the bleach features recorded shortly after the laser pulse (20 ps) do not show the distinctive pattern of the T and A bands expected if the complex were to bind at the terminal (TT/AA) base-pair site,[8f] but rather show major contributions from G and C.

The greater purine-dppz overlaps observed in the Λ-**1**-**I9**/**A9** crystals demonstrates how removal of the 2-amino group facilitates binding of the complex from the minor groove, as has been shown previously for minor-groove binding drugs.[5] The steady-state titrations reported above do indeed indicate that the complex binds with comparable strength to **I9** and **A9**, but much more weakly to **G9**.

Other guides to the nature of the binding at CG/CG and CA/TG steps (step **b** in the present work) are provided by our previous structural studies,[11e,j] in which we concluded that in both cases, angled intercalation from the minor groove led to stacking of one ancillary phen or TAP ligand onto the 3′ sugar on the purine side. Both the structural and the solution evidence presented here show that a CI/CG step is closely similar to a CA/TG step when binding to these lambda enantiomers. At these steps, the effect of the 2-NH_2 of guanine is again to displace the dppz chromophore and give reduced overlap, as highlighted in Figure 8 such that the pyrazine ring does not overlap directly with either guanine. At the CA/TG step, and therefore the CI/CG step, the absence of the 2-NH_2 substituent allows greater pyrazine-guanine overlap.

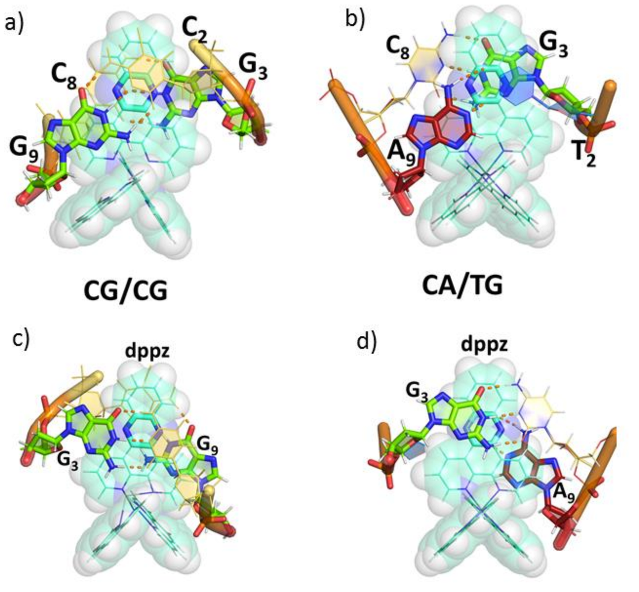

Figure 8. Structural models for the binding of the lambda complex at the second step of the duplexes, based on the isosteric Λ-$[Ru(phen)_2(dppz)]^{2+}$: PDB codes 5LFW (for a CG/CG step) and 4JD8 (for a CA/TG step).(a,b) G_9 above the dppz (c,d) G_3 above the dppz. Purine residues are shown as sticks and pyrimidine residues as lines. The central pyrazine ring of the dppz ligand is also shown as sticks.

Finally these studies also highlight that, as we found previously with $\{d(GC)_5\}_2$ and $\{d(G_5C_5)\}_2$,[8e] it is the lambda-enantiomer which appears to be much more sensitive to the sequence. As noted above, the angled configuration of the lambda-enantiomer at the 5’-pyrimidine -purine-3’ step causes it to interact with one of the purines. Conversely for the delta-species, as was observed upon binding to {dATGCAT}$_2$,[11e] angled binding in the intercalation pocket leads to overlap with one of the pyrimidines, on the 5'-side of the step (see Figure S20). Therefore, for such angled binding we would anticipate that the inosine-guanine substitution would not lead to an enhanced binding preference for the delta-complex – in agreement with what is found.

Conclusions

We have demonstrated that substitution of guanine for inosine in a DNA decamer significantly enhances the electron transfer for a bound Ru(II) photosensitiser in solution. This contrasts with the expectation from the crystal structure and the redox property of inosine. This is explained by the existence of a different binding site in solution CI/CG for **I9** due to the steric consequences in the minor groove of removal of the NH_2 group. This explanation is supported by the extent of PET, with G_3 as the most probable site of oxidation.

Our study also demonstrates that care needs to be taken in the use of inosine substitution as a control experiment for guanine oxidation by intercalating sensitisers. The similar electron transfer behaviour in both AT and IC systems, which are structurally similar from the minor groove but different from the major groove, offers further evidence that these Ru(II)dppz complexes intercalate preferentially from the minor groove in solution.[24] The enhancement in electron transfer highlights the role of base sequence in Ru(II)dppz binding, and demonstrates how the preferred binding sites in the crystal may differ from those in dilute solution. This supports the need to perform spectroscopic measurements in the crystal itself where structural and dynamics data can be directly correlated,[12] and where the high concentrations may approximate those in biological media.

Experimental Section

The synthesis of Λ-[Ru(TAP)$_2$(dppz)].2Cl was carried out by a modification to the method previously described by Elias *et al.*,[8b] and has been described in detail recently.[8e] Ps/ns-transient absorption and time-resolved infrared spectra were recorded on the ULTRA apparatus at the Rutherford Appleton Laboratories, which has been described in detail elsewhere.[25] X-ray data were recorded on beamline I02 at Diamond Light Source and were processed using a range of software (see ESI section S1 for full details).[26] Crystallographic coordinates and experimental data can be downloaded from www.wwpdb.org using PDB IDs 4QIO and 5ET2.

Acknowledgements

This work was supported by BBSRC grants BB/K019279/1 and BB/M004635/1, Royal Irish Academy/Royal Society exchange programme, STFC for programme access to the CLF (App 13230047), Laserlab-Europe for access to CLF (App 12240002), the School of Chemistry, UCD (SJQ), Science Foundation Ireland (SFI PI Awards 10/IN.1/B2999 and 13/IA/1865 to TG) and the Irish Research Council (FEP).

Keywords: DNA • electron transfer • inosine • minor groove • dppz • photo-oxidation • . ruthenium polypyridyl

[1] Inosine is the nucleoside of the hypoxanthine nucleobase, just as guanosine is the nucleoside of guanine. However, it is common to use inosine as the generic term and this has been followed in the current study.

[2] (a) N. Paz-Yaacov, E. Y. Levanon, E. Nevo, Y. Kinar, A. Harmelin, J. Jacob-Hirsch, N. Amariglio, E. Eisenberg, G. Rechavi, *Proc. Natl. Acad. Sci. U. S. A.* **2010**, *107*, 12174–12179; (b) I. Alseth, B. Dalhus, M.Bjøra, *Curr. Opin. Genetic Dev.* **2014**, *26*, 116–123; (c) K. Nishikura, *Annu. Rev. Biochem.* **2010**, *79*, 321–349; (d) B.-E. Wulff, M. Sakurai, K. Nishikura, *Nat. Rev. Genet.* **2011**, *12*, 81–85.

[3] F. H. Martin, M. M. Castro, F. Aboul-ela, I. Tinoco, Jr., *Nucleic Acids Res.* **1985**, *13*, 8927-8938.

[4] N. O. Reich, K. R. Sweetnam, *Nucleic Acids Res.* **1994**, *22*, 2089-2093

[5] (a) G. N. Bennett, Nucleic Acids Res., **1982**, *10*, 4581-4594; (b) P. L. Hamilton, D. P. Arya, *Nat. Prod. Rep.* **2012**, *29*, 134-143; (c) C. Bailly, D. Suh, M. J. Waring, J. B. Chaires, *Biochemistry* **1998**, *37*, 1033-1045; (d) C. Marchand, C. Bailly, M. J. McLean, S. E. Moroney, M. J.Waring, *Nucleic Acids Res.* **1992**, *21*, 5601-5606; (e) C. Bailly, M. J. Waring *Nucleic Acids Res.* **1995**, *23*, 885-892

[6] J. K. Barton, E. D. Olmon, P. A. Sontz, *Coord. Chem. Rev*. **2011**, *255*, 619-634; b) E. Wachter, D. K. Heidary, B. S. Howerton, S. Parkin, E. C. Glazer, *Chem. Commun.* **2012**, *48*, 9649–9651; c) M. R. Gill, J. A. Thomas, *Chem. Soc. Rev.* **2012**, *41*, 3179-3192; d) A. M. Palmer, S. J. Burya, J. C. Gallucci, C. Turro, *ChemMedChem* **2014**, *9*, 1260–1265; e) L. Marcélis, C. Moucheron, A. Kirsch – De Mesmaeker, *Phil. Trans. R. Soc. A* **2013**, 20120131; f) C. Hiort, P. Lincoln, B. Norden, *J. Am. Chem. Soc.* **1993**, *115*, 3448-3454; g) A. W. McKinley, P. Lincoln, E. M. Tuite, *Coord. Chem. Rev.* **2011**, *255*, 2676– 2692

[7] F. E. Poynton, J. P. Hall, P. M. Keane, C. Schwarz, I. V. Sazanovich, M. Towrie, T. Gunnlaugsson, C. J. Cardin, D. J. Cardin, S. J. Quinn, C. Long, J. M. Kelly, *Chem. Sci.* **2016**, *7*, 3075-3084 and references therein.

[8] a) C. G. Coates, P. Callaghan, J. J. McGarvey, J. M. Kelly, L. Jacquet, A. Kirsch-De Mesmaeker, *J. Mol. Struc.* **2001**, *598*, 15-25; b) I. Ortmans, B. Elias, J. M. Kelly, C. Moucheron, A. Kirsch-DeMesmaeker, *Dalton Trans.*, **2004**, 668-676; c) B. Elias, C. Creely, G. W. Doorley, M. M. Feeney, C. Moucheron, A. Kirsch - DeMesmaeker, J. Dyer, D. C. Grills, M. W. George, P. Matousek, A. W. Parker, M. Towrie, J. M. Kelly, *Chemistry – Eur. J*. **2008**, *14*, 369-375; d) J. A. Smith, M. W. George, J. M. Kelly, *Coord. Chem. Rev.* **2011**, *255*, 2666–2675; e) P. M. Keane, F. E. Poynton, J. P. Hall, I. P. Clark, I. V. Sazanovich, M. Towrie, T. Gunnlaugsson, S. J. Quinn, C. J. Cardin, J. M. Kelly, *J. Phys. Chem. Lett.* **2015**, *6*, 734-738; f) P. M. Keane, F. E. Poynton, J. P. Hall, I. V. Sazanovich, M. Towrie, T. Gunnlaugsson, S. J. Quinn, C. J. Cardin, J. M. Kelly, *Angew. Chem. Int. Ed.* 2015, **29**, 8364-8368; *Angew. Chem.* **2015**, *127*, 8484-8488; g) P. M. Keane, F. E. Poynton, J. P. Hall, I. P. Clark, I. V. Sazanovich, M. Towrie, T. Gunnlaugsson, S. J. Quinn, C. J. Cardin, J. M. Kelly, *Faraday Discuss.* **2015**, *185*, 455-469.

[9] L. Jacquet, R. J. H. Davies, A. Kirsch-De Mesmaeker, J. M. Kelly, *J. Am. Chem. Soc.* **1997**, *119*, 11763–11768.

[10] S. M. Cloonan, R. B. P. Elmes, M. Erby, S. A. Bright, F. E. Poynton, D. E. Nolan, S. J. Quinn, T. Gunnlaugsson, D C Williams, *J. Med. Chem.* **2015**, *58*, 4494-4505

[11] a) J. P. Hall, K. O'Sullivan, A. Naseer, J. A. Smith, J. M. Kelly, C. J. Cardin, *Proc. Natl. Acad. Sci. U. S. A.*, **2011**, *108*, 17610-17614; b) H. Niyazi, J. P. Hall, K. O'Sullivan, G. Winter, T. Sorensen, J. M. Kelly, C. J. Cardin, *Nat. Chem.* **2012**, *4*, 621-628; c) J. P. Hall, H. Beer, K. Buchner, D. J. Cardin, C. J. Cardin, *Phil. Trans. R. Soc. A* **2013**, *371*, 20120525-20120532; d) H. Song, J. T. Kaiser, J. K. Barton, *Nat. Chem.* **2012**, *4*, 615-620; e) J. P. Hall, D. Cook, S. R. Morte, P. McIntyre, K. Buchner, H. Beer, D. J. Cardin, J. A. Brazier, G. Winter, J. M. Kelly, C. J. Cardin, *J. Am. Chem. Soc.* **2013**, *135*, 12652-12659; f) J. P. Hall, H. Beer, K. Buchner, D. J. Cardin, C. J. Cardin, *Organometallics* **2015**, *34*, 2481-2486; g) D. R. Boer, L. Wu, P. Lincoln, M. Coll, *Angew. Chem. Int. Ed.* **2016**, *53*, 1949-1952; h) J. P. Hall, J. Sanchez-Weatherby, C. Alberti, C. H. Quimper, K. O'Sullivan, J. A. Brazier, G. Winter, T. Sorensen, J. M. Kelly, D. J. Cardin, C. J. Cardin, *J. Am. Chem. Soc.* **2014**, *136*, 17505–17512; i) J. P. Hall, P. M. Keane, H. Beer, K. Buchner, T. L. Sorensen,

10.1002/chem.201701447

D. J. Cardin, J. A. Brazier, C. J. Cardin, *Nucleic Acids Res.* **2016**, *44*, 9472-9482; j) J. P. Hall, S. P. Gurung, J. Hendle, P. Poidl, J. Andersson, P. Lincoln, G. Winter, T. Sorensen, D. J. Cardin, J. A. Brazier, C. J. Cardin, *Chem. - Eur. J*. **2017**, *23,* 4981-4985; k) C. J. Cardin, J. M. Kelly, S. J. Quinn, *Chem. Sci.,* 2017, DOI: 10.1039/ c7sc01070b

[12] J. P. Hall, F. E Poynton, P. M. Keane, S. P. Gurung, J. A. Brazier, D. J. Cardin, G. Winter, T. Gunnlaugsson, I. V. Sazanovich, M. Towrie, C. J. Cardin, J. M. Kelly, S. J. Quinn, *Nat. Chem.* **2015**, *7*, 961-967

[13] a) S. O. Kelley, J. K. Barton, *Science* **1999**, *238*, 375-381; b) C. Wan, T. Fiebig, O. Schiemann, J. K. Barton, A. H. Zewail, *Proc. Natl. Acad. Sci. U. S. A.* **2000**, *97*, 14052-14057; c) M. F. Sistare, S. J. Codden, G. Heimlich, H. H. Thorp, *J. Am. Chem. Soc.* **2000**, *122*, 4742-4749; d) F. Shao, M. A. O'Neill, J. K. Barton, *Proc. Natl. Acad. Sci. U. S. A.* **2004**, *101*, 17914-17919.

[14] a) M. T. Carter, M. Rodriguez, A. J. Bard, *J. Am. Chem. Soc.* **1989**, *111*, 8901-8911; b) B. C. Poulsen, S. Estalayo-Adrián, S. Blasco, S. A. Bright, J. M. Kelly, D. C. Williams, T. Gunnlaugsson, *Dalton Trans.* **2016**, *45*, 18208-18220

[15] I. Haq, J. E. Ladbury, B. Z. Chowdhry, T. C. Jenkins, J. B. Chaires, *J. Mol. Biol.* **1997**, *21*, 244-257.

[16] A. K. F. Martensson , P. Lincoln, *Dalton Trans.* **2015**, *44***,** 3604-3613 and refs therein..

[17] Comparative ps-TrA experiments were performed on Λ-**1** in the presence of either **G9** (see ref. 8e) or **I9** at [Ru]/[duplex] ratios of 0.2, 0.4, 0.8, 1.6 and 3.2. The presence of unbound species became apparent only above a 1:1 ratio. Single exponential fits of the forward ET were the same within error at [Ru]/[duplex] = 0.2, 0.8 and 3.2 (ESI Fig. S9 and Table S3)

[18] Transient experiments were performed with Λ-**1** in the presence of poly{dI-dC}$_2$, in order to confirm that inosine in a double stranded polymer does not quench Λ-**1**. There was no evidence for electron transfer and the excited state lifetime of 1500 ns is similar to that reported in the presence of poly{dA-dT}$_2$, and longer than that reported for unbound **1** (*ca.* 1 µs, see ref 8b). (ESI Fig. S10)

[19] A. W. Parker, C. Y. Lin, M. W. George, M. Towrie, M. K. Kuimova, *J. Phys. Chem. B* **2010**, *114*, 3660-366

[20] Q. Cao, C. M. Creely, J. Dyer, T. L. Easun, D. C. Grills, D. A. McGovern, J. McMaster, J. Pitchford, J. A. Smith, X.-Z. Sun, J. M. Kelly, M. W. George, *Photochem. Photobiol. Sci.* **2011**, *10*, 1355-1364

[21] M. Banyay, M. Sarkar, A. Graslund, *Biophys. Chem.* **2003**, *104*, 477 – 488

[22] E. Protozanova, P. Yakovchuk, M. D. Frank-Kamenetskii, *J. Mol. Biol.* **2004**, *342*, 775-785

[23] a) I. Saito, T. Nakamura, K. Nakatani, Y. Yoshioka, K. Yamaguchi, H. Sugiyama, *J. Am. Chem. Soc.* **1998**, *120*, 12686-12687; b) Y. A. Lee, A. Durandin, P. C. Dedon, N. E. Geacintov, V. Shafirovich *J Phys Chem B.* **2008**, *112*, 1834–1844.

[24] a) E. Tuite, P. Lincoln, B. Nordén, *J. Am. Chem. Soc.* **1997**, *119*, 239-240; b) A. Greguric, I. D. Greguric, T. W. Hambley, J. R. Aldrich-Wright, J. G. Collins, *Dalton Trans.* **2002**, *6*, 849-855; (c) J. G. Collins, A. D. Sleeman, J. R. Aldrich-Wright, I. Greguric, T. W. Hambley, *Inorg. Chem.* **1998**, *37*, 3133-3141.

[25] a) G. M. Greetham, P. Burgos, Q. Cao, I. P. Clark, P. S. Codd, R. C. Farrow, M. W. George, M. Kogimtzis, P. Matousek, A. W. Parker, M. R. Pollard, D. A. Robinson, Z. J. Xin, M. Towrie, *Appl. Spectrosc.* **2010**, *64*, 1311-1319; b) G. M. Greetham, D. Sole, I. P. Clark, A. W. Parker, M. R. Pollard, M. Towrie, *Rev. Sci. Instrum.* **2012**, *83*, 103-107.

[26] a) G. Winter, C. M. C. Lobley, S. M. Prince, *Acta Crystallogr.* **2013** *D69*, 1260-1273; b) W. Kabsch, *Acta Crystallogr.* **2010**, *D66*, 125-132; c) G. M. Sheldrick, *Acta Crystallogr.* **2008**, *A64*, 112-122; d) Collaborative Computational Project Number 4, *Acta Crystallogr.* **1994**, *D50*, 760-763; e) G. N. Murshudov, A. A. Vagin, E. J. Dodson, *Acta Crystallogr.* **1997**, *D53*, 240-255; f) P. Emsley, B. Lohkamp, W. G. Scott, K. Cowtan. *Acta Crystallogr.* **2010**, *D66*, 486-501.

10.1002/chem.201701447

FULL PAPER

Entry for the Table of Contents (Please choose one layout)

Layout 1:

FULL PAPER

Replacement of guanine by inosine in a sequence of DNA results in an unexpected increase in electron transfer by a bound Ru(II) complex. The effect is explained by a change in the binding of the complex due to the removal of an amino group from the minor groove of the DNA

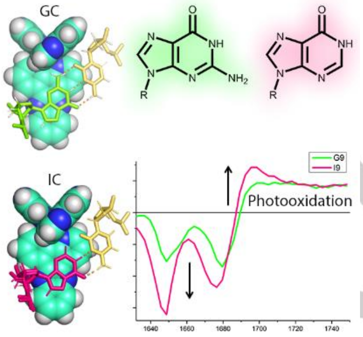

Páraic M. Keane, James P. Hall, Fergus E. Poynton, Bjørn C. Poulsen, Sarah P. Gurung, Ian P. Clark, Igor V. Sazanovich, Michael Towrie, Thorfinnur Gunnlaugsson, Susan J. Quinn,* Christine J. Cardin,* John M. Kelly**

Page No. – Page No.

Inosine can increase DNA's susceptibility to photo-oxidation by a Ru(II) complex due to the structural change in the minor groove.

Layout 2:

FULL PAPER

((Insert TOC Graphic here; max. width: 11.5 cm; max. height: 2.5 cm))

*Author(s), Corresponding Author(s)**

Page No. – Page No.

Title

Text for Table of Contents